Catalytic decomposition of dialkyl pyrocarbonates to dialkyl carbonates and carbon dioxide in dichloromethane by a discrete cobalt(II) alkoxide species generated *in situ*†

Bryan Greener and Paul H. Walton*

*Department of Chemistry, University of York, Heslington, York, UK YO1 5DD*

Dimethyl pyrocarbonate (dmpc) [dimethyl μ-oxo-bis(dioxocarbonate)] and diethyl pyrocarbonate (depc) were catalytically decomposed to dimethyl and diethyl carbonate respectively and carbon dioxide in the presence of [CoL(OR)]⁺ [L = *cis,cis*-1,3,5-tris(*E,E*-cinnamylideneamino)cyclohexane, R = methyl or ethyl] which we propose to be generated *in situ* during reaction in dichloromethane. The activity of the catalyst is undiminished after 60 000 turnovers. In both cases the catalytic rate enhancement for the decomposition is in excess of 10^7 dm³ mol⁻¹ of catalyst. The catalytic process follows Michaelis–Menten type kinetics and k_{obs} is 2.2(2) s⁻¹ for dmpc decomposition and 1.3(2) s⁻¹ for depc decomposition. Activation energies for the catalytic decomposition are E_{dmpc} = 113(5) and E_{depc} = 120(11) kJ mol⁻¹. A mechanism involving cobalt-bound alkoxide attack on dialkyl pyrocarbonate is proposed. The crystal structure of [CoL(Cl)] BPh₄ has been determined by single-crystal X-ray diffraction.

Early transition-metal alkoxides have long been used as catalysts or reagents in organic reactions.[1] In contrast, simple alkoxide (methoxide, ethoxide) complexes of later transition metals are uncommon[2] and mostly restricted to pendant alcohol deprotonation.[3,4] In particular, Co^{II}–OR (R = Me or Et) complexes are rare. The compounds Co(OMe)₂ and Co(OEt)₂ are inert, polymeric materials,[5] and there is only one report of a soluble, monomeric Co^{II}–OR (R = Me or Et) complex.[6] Accordingly, we have focused our recent studies on the preparation of discrete Co^{II}–OMe and Co^{II}–OEt complexes. Such complexes have the potential to act as effective alkoxide-based catalysts or reagents in organic solvents, due to their relatively high ligand-exchange rates and the small stability differences between four- and six-co-ordinate complexes.[7] [Several Co^{III}–OR (R = Me or Et) complexes have been characterised,[8] but none is reported to act as a catalyst or reagent, presumably due, in part, to the low ligand-exchange rates.] Furthermore, a discrete complex has advantages insofar as its mechanism of action can be studied more easily than non-discrete species.[9] For example, Chisholm and Eilert[10] recently used a hindered tris(pyrazolyl)borate magnesium alkoxide complex to catalyse the synthesis of poly(dilactide). By using such a discrete, monomeric species they were able to propose a mechanistic sequence for the ring-opening polymerisation.

We have adopted a similar approach to that of Chisholm and Eilert to produce a face-capping ligand that was able to form a soluble, monomeric, ligand–cobalt(II)–alkoxide complex. We decided against the use of a tris(pyrazolyl)borate ligand as we were aware of the limitations of a negatively charged ligand in terms of the complex's ability to stabilise a negatively charged substrate. In view of the general instability of alkoxides, we thought it would be desirable to produce the active species, when required, *in situ*. Furthermore, to produce a catalytic alkoxide species we would also have to disfavour co-ordinative saturation at the metal,[11] but at the same time allow flexibility in the metal's co-ordination number. To meet these goals, in this study, we prepared the neutral, hydrophobic molecule *cis,cis*-1,3,5-tris(*E,E*-cinnamylideneamino)cyclohexane L, see Scheme 1, and its complexes CoL(X)(H₂O)$_n$(BPh₄) where X = ClO₄ **1**,
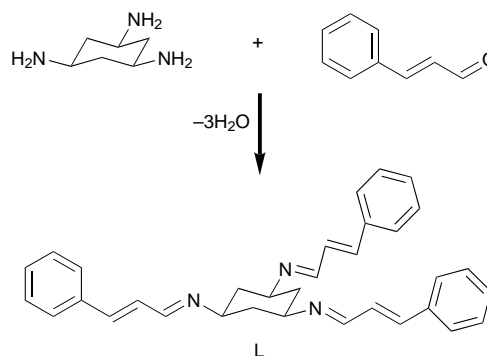
**Scheme 1** Condensation of *cis,cis*-1,3,5-triaminocyclohexane with cinnamaldehyde to give L
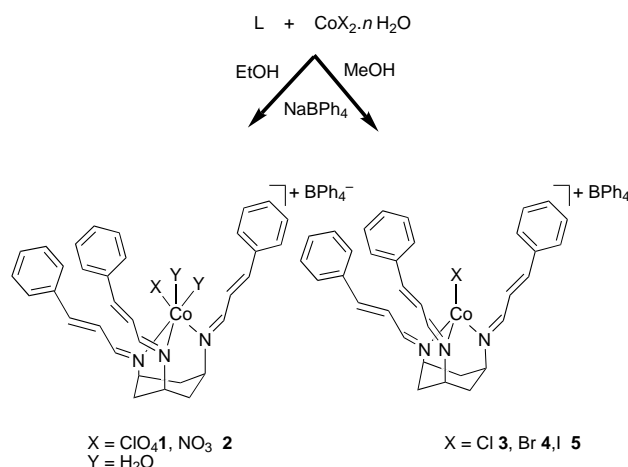
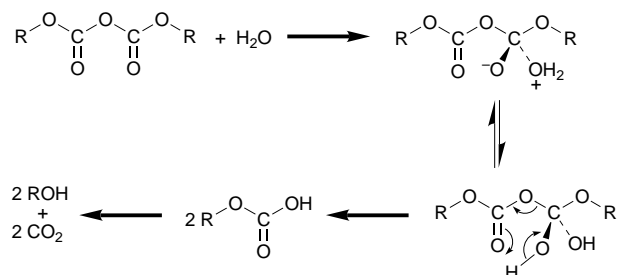**Scheme 2** Complexation of L with metal salts

NO₃ **2**, Cl **3**, Br **4** or I **5**, see Scheme 2. Previous metal complexes of L demonstrate an N₃ face-capping geometry and a rigid hydrophobic cavity that surrounds the metal's remaining co-ordination sites.[12] This cavity prevents polymerisation of the [CoL(OR)]⁺ species *via* alkoxide bridging and makes the complexes lipophilic enough to be soluble in organic solvents; complexes of L are highly soluble in dichloromethane. To generate

X = ClO₄ **1**, NO₃ **2**
Y = H₂O
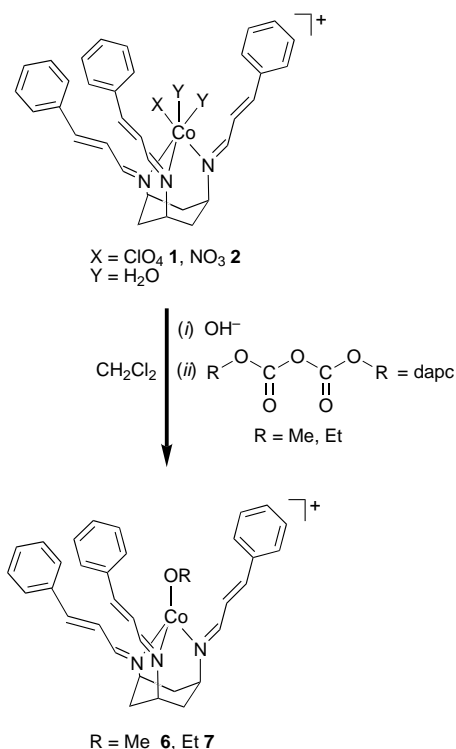
Scheme 3 Generation of compounds **6** and **7** from reaction of **1** and **2** with sodium hydroxide followed by dapc

Scheme 4 Proposed mechanism of dapc hydrolysis in water [17]

Fig. 1 An ORTEP [21] diagram, showing 50% probability thermal ellipsoids, of complex **3** (BPh₄ omitted for clarity)

Fig. 2 Comparison of solid-state (KBr disc), top, and solution (CH₂Cl₂), bottom, IR spectra of complex **3**. Detector saturation bands due to CH₂Cl₂ are marked with an asterisk

the desired alkoxide intermediate [CoL(OR)]⁺ where R = Me **6** or Et **7**, we treated a dichloromethane solution of **1** or **2** with solid sodium hydroxide to give [CoL(OH)]⁺ **8** *in situ* (analogous metathesis reactions have been carried out previously [13]). An appropriate dialkyl pyrocarbonate (dapc) [dialkyl μ-oxo-bis(dioxocarbonate)] was then added to this solution, dimethyl pyrocarbonate (dmpc) to generate **6** and diethyl pyrocarbonate (depc) to generate **7**, see Scheme 3.

Dialkyl pyrocarbonates have been employed for several decades as carboxylating agents in enzyme-inhibition studies.[14] More recently they have found applications in food and beverage preservation,[15] in batteries[16] and as precursors to (alkyl carbonato)metal complex formation.[17,18] They are unstable in the presence of water and hydrolyse to form carbon dioxide and alcohol; the mechanism in Scheme 4 has been proposed for this process.[19] Their decomposition has also been studied in ethanol, where it occurs extremely slowly yielding dialkyl carbonate and carbon dioxide.[20] The reactivity of dapcs in other solvents has not been studied and, to our knowledge, they have not been used as alkylating agents. There have not been any previous studies of catalytic dapc decomposition.

In this study we demonstrate that monomeric [Co–OR]⁺ complexes can be prepared by using a neutral, sterically demanding ligand. The resulting complexes are catalytically active in the decomposition of dapc, with remarkably high catalytic rate enhancements for the decomposition; in excess of 10⁷ per mol dm⁻³ catalyst, with activation energies in excess of 100
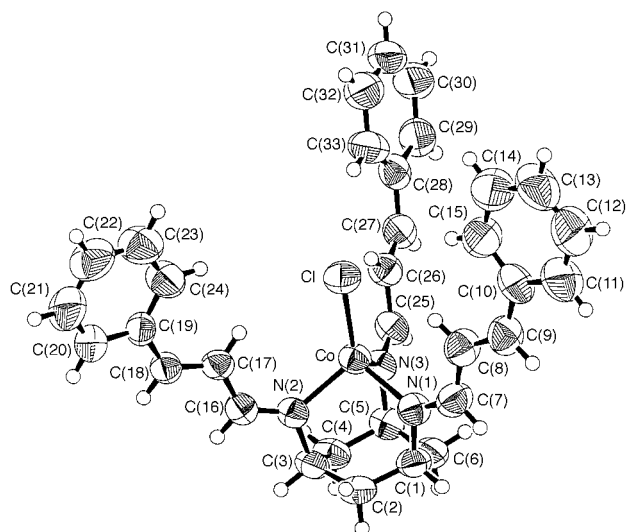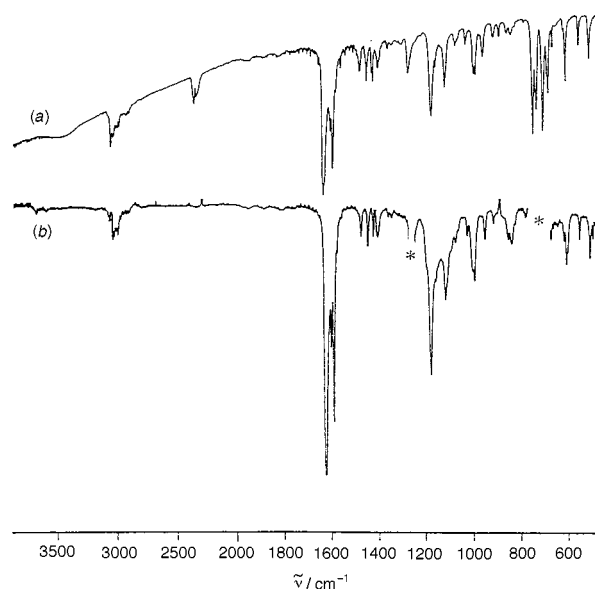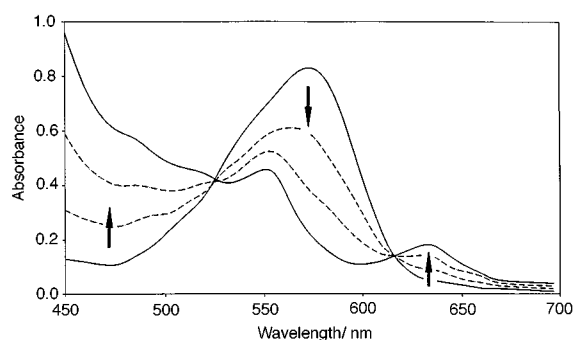
kJ mol⁻¹. The complexes are also very robust with respect to degradation during turnover, catalysing >60 000 turnovers per catalyst molecule. We have also been able to measure the relative rates of [Co–OMe]⁺ and [Co–OEt]⁺ reaction with dapc, showing the methoxide species to be approximately twice as reactive as the ethoxide species. To our knowledge, these are the first catalytically active [Co–OR]⁺ species, demonstrating the successful use of a sterically demanding ligand to control metal co-ordination numbers and stabilise discrete, monomeric [Co–OR]⁺ species.

Results and Discussion

Compound L was synthesized by condensation of *cis,cis*-1,3,5-triaminocyclohexane with 3 equivalents of cinnamaldehyde [12] (Scheme 1). The complexes **1**–**5** were prepared by the combination of L with the appropriate metal salt followed by addition of sodium tetraphenylborate (Scheme 2). All except **5** were air-stable compounds. All were fully characterised by UV/VIS, IR, mass spectra and elemental analysis and the structure of **3** was determined by single-crystal X-ray diffraction (Fig. 1, selected

Table 1 Bond lengths (Å) and angles (°) for complex **3**

Co–N(1)	1.998(4)	C(18)–C(19)	1.457(7)
Co–N(2)	2.001(4)	C(19)–C(20)	1.396(7)
Co–N(3)	2.014(4)	C(20)–C(21)	1.390(8)
Co–Cl	2.203(2)	C(21)–C(22)	1.364(8)
N(2)–C(16)	1.276(5)	C(22)–C(23)	1.357(8)
C(16)–C(17)	1.432(6)	C(23)–C(24)	1.368(7)
C(17)–C(18)	1.326(6)	C(24)–C(19)	1.380(7)
N(1)–Co–Cl	119.63(13)	C(16)–C(17)–C(18)	121.9(5)
N(2)–Co–Cl	121.09(12)	C(17)–C(18)–C(19)	126.6(5)
N(3)–Co–Cl	122.77(13)	C(18)–C(19)–C(20)	118.7(5)
N(1)–Co–N(2)	99.7(2)	C(19)–C(20)–C(21)	120.6(6)
N(1)–Co–N(3)	93.2(2)	C(20)–C(21)–C(22)	120.1(6)
N(2)–Co–N(3)	95.3(2)	C(21)–C(22)–C(23)	119.8(7)
Co–N(2)–C(16)	131.0(3)	C(22)–C(23)–C(24)	120.6(6)
N(2)–C(16)–C(17)	124.3(5)	C(23)–C(24)–C(19)	121.8(6)

Fig. 4 Second-order plot for uncatalysed decomposition of dmpc (●) and depc (■) in dichloromethane at room temperature

Fig. 3 The UV/VIS absorbance spectrum [at 293.0(5) K] during reaction of a dichloromethane solution of complex **1** (λ_{max} = 575 nm) with NaOH. Broken lines show intermediate stages during the conversion. Conversion is complete in *ca.* 10 min

bond lengths and angles in Table 1). The structure demonstrates the expected face-capping co-ordination of L and a rigid, hydrophobic cavity around the metal's remaining co-ordination sites. The cobalt co-ordination geometry is approximately C_{3v} with a chloride anion occupying the axial position. The cavity formed by L favours four- over six-co-ordination and disfavours the formation of LM–X–ML species, where X is a single atom.‡ From IR studies in solution (CH_2Cl_2) and the solid-state (KBr disc), see Fig. 2, we conclude that this general solid-state structure persists in solution for **1–5**. The UV/VIS spectra, in dichloromethane, of **1–5** all exhibit d–d transitions with absorption coefficients of greater than 300 dm^3 mol^{-1} cm^{-1}. The solid-state infrared spectra (500–4000 cm^{-1}) of **1** and **2** have broad bands at 3400–3600 cm^{-1}, indicative of the presence of water. In contrast, those of **3–5** are identical and are free of water bands.

From these results we propose that complexes **1–5** are four-co-ordinate in the solid state and in dichloromethane while **1** and **2** are hydrated and probably six-co-ordinate in the solid state.§ {We propose **1** and **2** to be $[CoL(H_2O)_2(ClO_4)]BPh_4$ and $[CoL(H_2O)_2(NO_3)]BPh_4$ respectively, consistent with elemental analysis.} Analogues of compounds **1–5** could not be prepared from L when its imine bonds had been reduced to alkylamine with $NaBH_4$ (L was reduced in methanol with $NaBH_4$ using the method in ref. 23). This may imply that the cavity plays a role in stabilising discrete species such as **1–5**.

When a solution of complex **1** or **2** in dichloromethane was shaken with solid sodium hydroxide a change in the UV/VIS spectrum was observed, see Fig. 3, with the isosbestic evolution
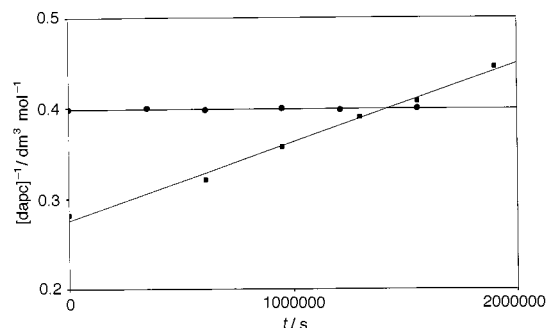
of a common species (λ_{max} = 551 nm, ε = 430 dm^3 mol^{-1} cm^{-1}) from both precursors. In the positive-ion FAB mass spectrum, the $[CoL(ClO_4)]^+$ m/z = 629 or $[CoL(NO_3)]^+$ m/z = 592 peak was lost with the concomitant appearance of a peak, m/z = 547, consistent with the formation of $[CoL(OH)]^+$ **8**. This species could not be isolated but exposure of this solution to carbon dioxide produced a purple precipitate which was fully characterised as the bridged dimer $[(CoL)_2(\mu\text{-}CO_3)][BPh_4]_2$ **9**.¶ Identical chemistry has been observed in equivalent tris(pyrazolyl)-borate complexes.[24]

The complexes **1–5** and **8** were used in reactivity studies where the rate of dapc decomposition was followed by measuring the rate of carbon dioxide evolution. At room temperature, in the absence of catalyst, dmpc and depc decomposed to dimethyl and diethyl carbonate respectively and carbon dioxide in dichloromethane; these processes were extremely slow with second-order rate constants of $6(9) \times 10^{-10}$ (dmpc) and $8.7(4) \times 10^{-8}$ dm^3 mol^{-1} s^{-1} (depc), see Fig. 4. A 1:1 molar ratio solution of dmpc and depc in dichloromethane decomposes, at the same rate, to dimethyl and diethyl carbonate, ethyl methyl carbonate and carbon dioxide. The presence of ethyl methyl carbonate confirms the second-order nature of the decomposition. It was impractical to follow a room-temperature reaction to completion but refluxing a 1:1 molar mixture of dmpc and depc at 200 °C for 24 h converted all dapc to dialkyl carbonate and ethyl methyl carbonate. From ^1H NMR spectroscopy the final product distribution was found to be 1:1:2 (molar ratio) for $(MeO)_2CO$, $(EtO)_2CO$ and $(MeO)(EtO)CO$ respectively. The presence of the latter in this proportion implies an intermolecular decomposition, which must occur *via* a bimolecular pathway. This is consistent with the observed kinetics.

Combination of the hydroxide complex $[CoL(OH)]^+$ with dapc in dichloromethane at room temperature resulted in a species which was observed by UV/VIS spectroscopy (549 nm with dmpc, 548 nm with depc, ε = 360 dm^3 mol^{-1} cm^{-1}) and resonance-Raman spectroscopy [dmpc, ν(C–O) 917, ν(Co–O) 521; depc, ν(C–O) 901, ν(Co–O) 520 cm^{-1}], see Fig. 5. This species is $[CoL(OR)]^+$ where R = Me or Et for dmpc and depc respectively, and this is supported by loss from the positive-ion FAB mass spectrum of the molecular ion peak from $[CoL(OH)]^+$ with the concomitant appearance of $[CoL(OR)]^+$ peaks, m/z = 561 and 575. {Note: in other experiments, these peaks were of equal intensity to those arising from an authentic sample of $[CoL(Cl)]^+$ present in solution at the same concentration, indicating that $[CoL(OMe)]^+$ and $[CoL(OEt)]^+$ were the major species in solution.}

Following the initial formation of $[CoL(OMe)]^+$ or $[CoL(OEt)]^+$, catalytic decomposition of dapc to dialkyl carbonate and CO_2 commenced. Kinetic and thermodynamic parameters for the overall catalytic process were determined by

‡ We have synthesized and characterized a wide range of transition-metal complexes with L and have not observed species of the type LM–X–ML, where X is a single atom.
§ We have structurally characterized octahedral complexes of L and of similar ligands.[22]

¶ Complex **9** has been fully characterised and will be the subject of a future publication. Concise crystallographic information is available as supplementary data.
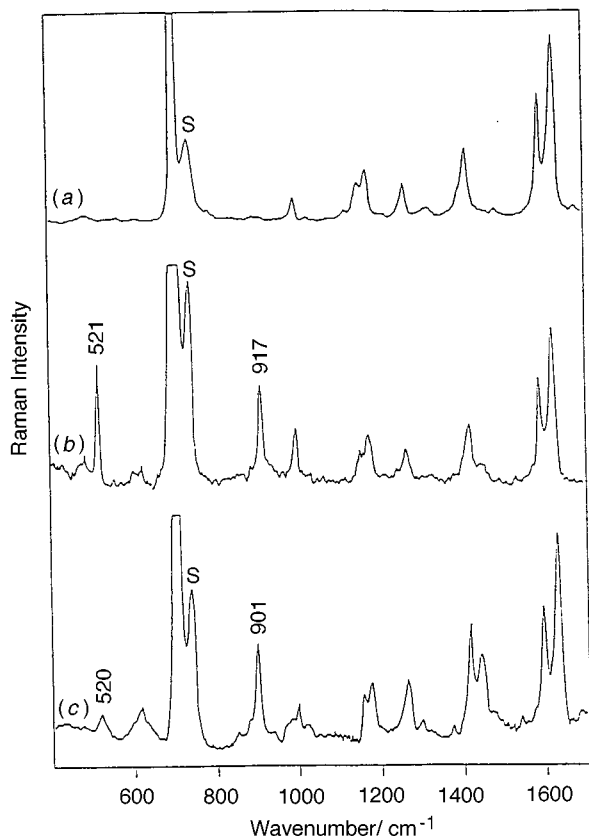
Fig. 6 Carbon dioxide evolution with time for catalysed reactions to determine k_{obs}

Fig. 7 Variation of the rate of CO_2 evolution with respect to complex concentration, for the catalytic conversion of dapc into dialkyl carbonate and CO_2 {at 293.0(5) K, [dmpc] = 3.0 (●), [depc] = 2.9 mol dm^{-3} (■)}

Fig. 5 Resonance-Raman spectra (S = solvent) of (*a*) complex **8** in dichloromethane, (*b*) after addition of dmpc and (*c*) after addition of depc. Excitation by argon-ion laser at 514.5 nm (50 mW)
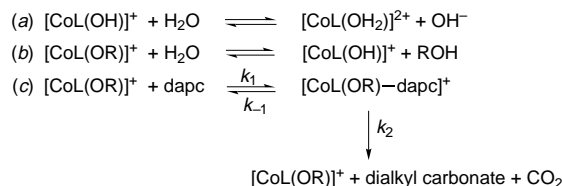
Scheme 5 Possible pre-reaction steps (*a*) and (*b*). (*c*) Proposed kinetics of catalysed reaction (analogous to Michaelis–Menten kinetics). When dapc is in great excess, [dapc] is effectively constant and so d[CO$_2$]/d$t = k_{obs}$[CoL(OR)$^+$]$_T$ where [CoL(OR)$^+$]$_T$ is the total complex concentration and $k_{obs} = k_2$[dapc]/(K + [dapc]) where $K = (k_{-1} + k_2)/k_1$ and is analogous to the Michaelis constant. Also $1/k_{obs} = (K/k_2[\text{dapc}]) + 1/k_2$

measuring the volume of carbon dioxide produced during decomposition. All reactions produced an approximately 1:1 stoichiometric volume of carbon dioxide with respect to dapc when complete; a slight shortfall in carbon dioxide was observed in all cases, equivalent to the quantity necessary for the formation of the dimeric complex **9**.

The kinetics observed was consistent with the model as shown in Scheme 5(*c*) (analogous to Michaelis–Menten enzyme kinetics). Catalytic rate constants, k_{obs} [see Scheme 5(*c*)], were determined with a 1000-fold molar excess of dapc over complex ([dmpc] = 2.79, [depc] = 3.55 mol dm^{-3}). Plots of CO_2 evolved over time are shown in Fig. 6. It can be seen that there is an increasing lag time, before the maximum steady rate, at low complex concentrations. This could be due to a small quantity of water present in the solvent protonating an appreciable quantity of **8** at low concentration and making the formation of **6** or **7** rate determining. The presence of water may also cause hydrolysis of **6** or **7** to give **8** [see Scheme 5(*a*) and (*b*)]. At low complex concentration formation of **6** or **7** is likely, therefore, to be rate determining. These reactions help to explain the non-zero intercepts in Fig. 7. At higher complex concentrations water is quickly consumed in the initial lag phase of the reac-
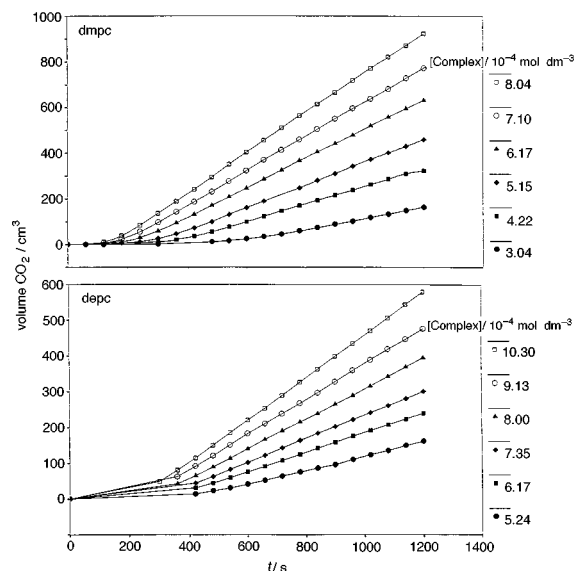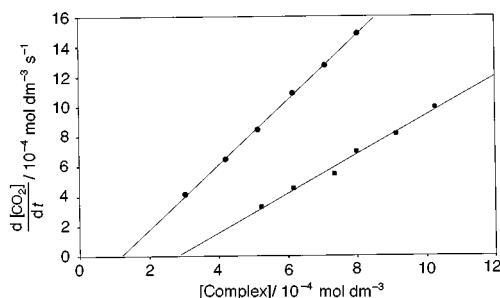
tion, after which the reaction proceeds according to standard kinetics. From a plot of decomposition rate *versus* complex concentration, dmpc decomposed with a rate constant, $k_{obs(dmpc)} = 2.2(2)$ s^{-1} at 293 K and depc with a rate constant $k_{obs(depc)} = 1.3(2)$ s^{-1} at 293 K (Fig. 7).

The linear plots in Fig. 7 demonstrate that the rate is first order with respect to complex concentration over the experimental concentration range but also show that $k_{obs(dmpc)} \neq k_{obs(depc)}$. Catalytic activity is undiminished after 60 000 turnovers per catalyst molecule, with the maximum amount of substrate converted being 485 mmol in our experiments.

To verify the kinetics of reaction proposed in Scheme 5, experiments were carried out under conditions where [dapc] $\not> K$, such that maximum catalytic activity was not achieved and the observed rate constant, k_{obs}, varied with initial [dapc]. Plots of $(1/k_{obs})$ *versus* $(1/[\text{dapc}])$ were obtained to calculate k_2 and K (analogous to a Lineweaver–Burke plot) and are shown in Fig. 8. Linear plots were obtained for both substrates and k_2 was found to be 2.6(4) s^{-1} for dmpc and 1.03(6) s^{-1} for depc, within error of the k_{obs} values obtained when the complex was saturated; with $K_{(dmpc)} = 1.5(4)$ and $K_{(depc)} = 1.0(1)$ dm^3 mol^{-1}. Such high values for K suggest that k_2 is significant compared to k_{-1} and therefore $K \neq k_{-1}/k_1$ in this case.

When the catalysed reaction (complex concentration 1.0×10^{-5} mol dm^{-3}, 1000-fold excess dapc) was observed over a range of temperatures, the gas-evolution plots shown in Fig. 9 resulted. The temperature range was narrow (288–301 K) because at lower temperatures gas evolution became impractically slow to monitor by this method, while above 301 K interference was observed from solvent vapour (this theory was tested
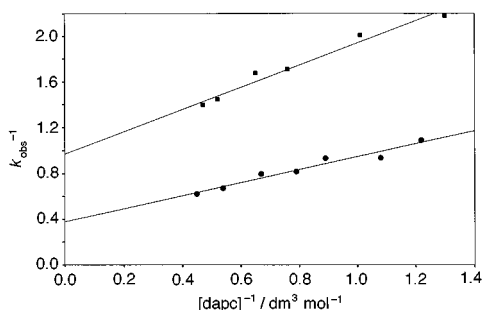
Fig. 8 Plot of $1/k_{obs}$ *versus* $1/[dapc]$ to determine K and k_2 [at 293.0(5) K]. Complex concentration 4.06×10^{-4} (dmpc, ●), 8.12×10^{-4} mol dm^{-3} (depc, ■). The dapc concentrations were in the range 0.82–2.22 mol dm^{-3} for dmpc and 0.79–2.13 mol dm^{-3} for depc
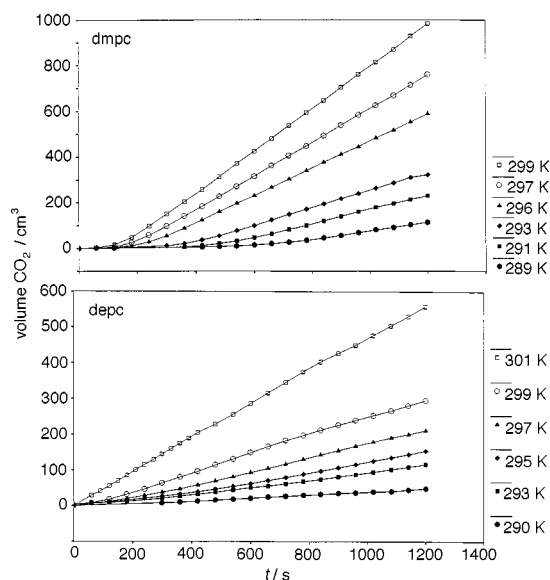

Fig. 11 Plot of reaction composition (% molarity) during the catalytic decomposition of a 1:1 molar mixture of dmpc (●) and depc (■) to $(MeO)_2CO$ (○), $(EtO)_2CO$ (□), $(MeO)(EtO)CO$ (△) and CO_2 [at 293.0(5) K] in CH_2Cl_2

Fig. 9 Carbon dioxide evolution with time over a range of temperatures for catalysed reactions to determine activation energy

Scheme 6 Proposed catalytic cycle for conversion of dapc into dialkyl carbonate and carbon dioxide in the presence of $[CoL(OR)]^+$. Step 1: attack on dapc by alkoxide; note the exchange of the alkoxide (this process has been highlighted by the use of bold and italic 'R'). We propose that the species shown in brackets is a likely intermediate for this process. The intermediate breaks down to generate a new alkoxide species and one molecule of dialkyl carbonate or $(MeO)(EtO)CO$, depending on substrate, and CO_2. Step 2: orientation of the next dapc molecule within the complex's hydrophobic cavity
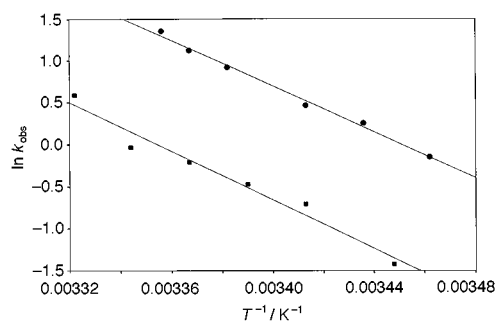

Fig. 10 Arrhenius plots for catalytic conversion of dapc into dialkyl carbonate and CO_2. *y* Intercepts: dmpc (●), 46(2); depc (■), 47(4). [dmpc] = 3.0, [depc] = 2.9 mol dm^{-3}, complex concentration 1.0×10^{-5} mol dm^{-3}

with a dichloromethane control experiment: below 301 K, no syringe movement was observed). Activation energies were determined, for these specific conditions, from plots of $\ln(k_{obs})$ against $1/T$ (Fig. 10): $E_{dmpc} = 113(5)$ kJ mol^{-1} and $E_{depc} = 120(11)$ kJ mol^{-1}.

An estimate of rate enhancements in the presence of catalyst can best be obtained by comparing rates of decomposition in the absence of catalyst and rates of decomposition, per mol dm^{-3} of catalyst, in the presence of catalyst. In catalysed reactions, [dmpc] = 3.0 and [depc] = 2.9 mol dm^{-3}, applying the second-order rate constants obtained from control reactions, involving dmpc and depc, leads to uncatalysed rates of
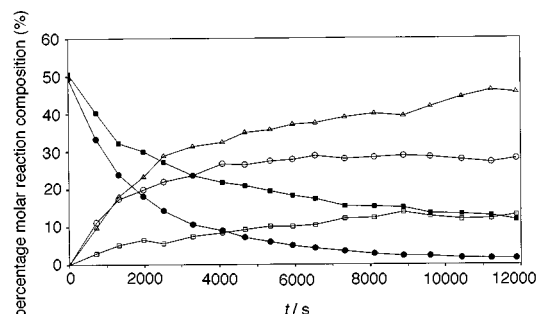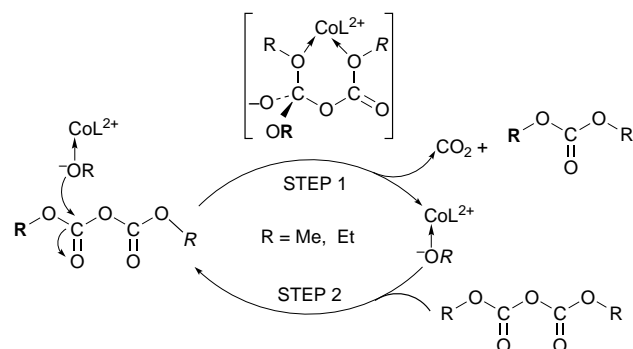
$5(1) \times 10^{-9}$ and $7.3(9) \times 10^{-8}$ mol dm^{-3} s^{-1}. Observed catalytic rates, per mol dm^{-3} catalyst, were 2.2(2) (dmpc) and 1.3(2) mol dm^{-3} s^{-1} (depc). Hence rate enhancements, per mol dm^{-3} catalyst, are of the order of 10^8 for dmpc and 10^7 for depc.

In the presence of complex **1** alone catalytic activity was observed but the rate of decomposition was approximately halved and there was a substantial lag time, *ca.* 15 min, before the maximum rate of decomposition was achieved (presumably **6** and **7** are more difficult to generate from **1** than **8**). In the presence of **2**–**5**, or in the presence of the metal salts $Co(ClO_4)_2 \cdot xH_2O$, $Co(BF_4)_2 \cdot xH_2O$, CoF_2, NaOH, NaOMe or NaOEt, the uncatalysed rate of dapc decomposition was not enhanced. [It was necessary to add a small quantity of methanol or ethanol (for dmpc and depc reactions respectively) to gain full solubility of the salts in dichloromethane.] The catalytic inactivity of **2**–**5** indicates that initial turnover to form **6** or **7** does not occur and this may be a consequence of these complexes being too inert to enable the reaction with dapc to be favourable.

To elucidate the catalytic cycle further, mixed substrate reactions were undertaken and followed by ^{1}H NMR spectroscopy; the cobalt(II) complex concentration was so low in comparison to that of substrate that it did not interfere with integration. The products and final product distribution were also confirmed by gas chromatography–electron impact (EI) mass spectrometry (GC-EIMS). The result is shown in Fig. 11. A 1:1 molar ratio solution of dmpc and depc was catalytically decomposed to carbon dioxide, $(MeO)_2CO$, $(EtO)_2CO$ and $(MeO)(EtO)CO$ with the product distribution molar ratio of $(MeO)_2CO + (EtO)_2CO : (MeO)(EtO)CO$ approximately equal to 1:1 (this is an approximation because, as demonstrated

Rate of reaction. R/ mol dm^{-3} s^{-1}
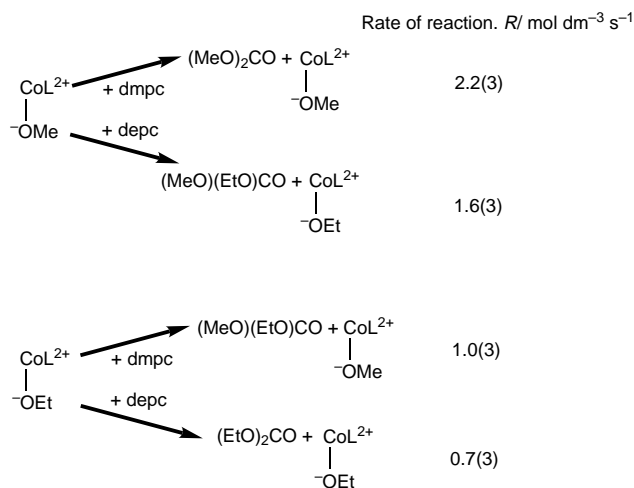
Scheme 7 Reaction pathways for the catalytic decomposition of a mixture of dmpc and depc to (MeO)$_2$CO, (EtO)$_2$CO and (MeO)(EtO)CO [at 293.0(5) K] and calculated rates of reaction for each pathway

above, the rate of dmpc decomposition is not equal to the rate of depc decomposition under the same conditions). From this product distribution we propose the mechanism shown in Scheme 6 for the catalytic process occurring in this study. The catalytic species, Co^{II}–OR$^+$, attacks a dapc molecule to produce carbon dioxide, dialkyl carbonate and regenerate a new catalytic species Co^{II}–OR$^+$ where R is dependent on the dapc molecule; during each catalytic cycle the alkoxide moiety is always exchanged.

From product distributions during early reaction (before 2000 s), approximate relative initial rates of dapc decomposition and dialkyl carbonate/(MeO)(EtO)CO formation could be determined: these rates could be calibrated by using an absolute rate constant, $k_{obs(dmpc)}$, which was earlier obtained from the single-substrate reaction studies; this value was found for dmpc conversion into (MeO)$_2$CO and CO$_2$. The resulting calibrated rate constants at 293 K are shown in Scheme 7: for **6**, $k_{dmpc} = 2.2(3)$ s^{-1} and $k_{depc} = 1.6(3)$ s^{-1}; for **7**, $k_{dmpc} = 1.0(3)$ s^{-1} and $k_{depc} = 0.7(3)$ s^{-1}. These rates show that **6** [Co–OMe]$^+$ is approximately twice as reactive as **7** [Co–OEt]$^+$, with respect to reaction with dmpc or depc. This can be explained in terms of complex stability, ethoxide being a better σ donor than methoxide, making attack on substrate less favourable in the first, and rate-determining, step of the proposed mechanism; however, steric effects may also be important.

Conclusion

We have successfully synthesized cobalt(II) complexes of a sterically hindered triimine ligand including a discrete, monomeric ligand–cobalt(II)–alkoxide species, which can be generated as required *in situ* in organic solvent. This type of ligand–cobalt(II)–alkoxide complex is the first of its kind and is also the first example of a catalytically active cobalt(II) alkoxide species. It catalyses the conversion of dialkyl pyrocarbonates into dialkyl carbonates and carbon dioxide. The rate enhancement for this process is in excess of 10^7 per mol dm^{-3} catalyst for dmpc and depc compared to the uncatalysed reaction and the reactivity of the catalyst is undiminished after 60 000 turnovers per catalyst molecule. As such, the catalyst is highly effective and robust to decomposition during turnover. The kinetic results imply that dapc is attacked by the cobalt-bound alkoxide within the complex's hydrophobic cavity. This cavity is also essential for the formation of discrete species such as **1–5**. The result of the mixed substrate reaction, with dmpc and depc, implies that the methoxide complex is a more reactive species than the ethoxide complex, with respect to reaction with dmpc or depc.

Experimental

Melting points were obtained using a standard Gallenkamp apparatus. The NMR spectra were acquired on a JEOL EX270MHz spectrometer, IR spectra using a Perkin-Elmer 1720 Fourier-transform spectrophotometer (KBr pellets pressed under 6.0 tonnes pressure), UV/VIS spectra using a Perkin-Elmer Lambda 15 spectrometer at 293(2) K, resonance-Raman spectra by excitation with an argon laser at 514.5 nm (50 mW) and collecting scattered light at 90° *via* a Spex 1403 double monochromator and Wright Instruments CCD detector and mass spectra on a Fisons Instruments Autospec using a 0–650 °C temperature range. Analyses were performed by Butterworth Laboratories Ltd., Teddington, Middlesex, England. Chemicals were used as received: dimethyl pyrocarbonate and diethyl pyrocarbonate from Aldrich Chemical Company Ltd. and dichloromethane from Fisons Ltd. Sodium methoxide and sodium ethoxide were prepared by standard procedures[1] from sodium and the corresponding alcohol.

Preparations

cis,cis-**1,3,5-Tris(*E,E*-cinnamylideneamino)cyclohexane L.** *cis, cis*-1,3,5-Triaminocyclohexane tris(dihydrogensulfate) (1.61 g, 3.8 mmol)[25] and sodium hydroxide (0.46 g, 11.5 mmol) were dissolved in water (10 cm^3) and to this a solution of cinnamaldehyde (1.51 g, 11.4 mmol) in diethyl ether (10 cm^3) was added. The mixture was stirred vigorously, in a sealed vessel for at least 3 h. The white precipitate was filtered off, washed with ether (50 cm^3) and desiccated until dry (0.88 g, 1.9 mmol, 49%), m.p. 184–187 °C, ^{1}H NMR (CD$_3$OD, 270 MHz): δ 8.30 (d, 3 H, $J = 9.0$, N=CH), 7.64 (m, 6 H, aryl), 7.49 (m, 9 H, aryl), 7.27 (d, 3 H, $J = 16.0$ Hz, PhC*H*=), 6.98 (dd, 3 H, $J = 16.0$, 9.0 Hz, =CHC*H*=CH), 3.60 (m, 3 H, CR$_2$*H*) and 1.90 (m, 6 H, CH$_2$). IR (KBr pressed pellet): 2950w, 2800w, 1632s, 1615m, 1449w, 1147w, 985m, 960w, 747s, 690s and 500w cm^{-1}. Positive-ion chemical ionisation mass spectrum: $m/z = 472$, $[M + H]^+$ [Found (Calc. for C$_{33}$H$_{33}$N$_3$): C, 83.65 (84.04); H, 6.70 (7.05); N, 8.62 (8.91)%].

[CoL(H$_2$O)$_2$(ClO$_4$)]BPh$_4$ 1. CAUTION!: perchlorate salts are potentially explosive. To a stirred solution of compound L (0.20 g, 0.4 mmol) and cobalt(II) perchlorate hexahydrate (0.15 g, 0.4 mmol) in ethanol (50 cm^3) was added dropwise a solution of sodium tetraphenylborate (0.14 g, 0.4 mmol) in ethanol (10 cm^3). The salmon pink precipitate was filtered off under vacuum, washed with ethanol (50 cm^3) and desiccated until dry, darkening to purple (0.36 g, 0.4 mmol, 91%), m.p. 136–137 °C. IR (KBr pressed pellet): 3600–3400s, 3060s, 1630s, 1590s, 1470m, 1455m, 1410m, 1255m, 1380s, 1315s, 1200–1100s, 750s, 745s, 680s, 675s, 605s, 550w and 505m cm^{-1}. UV/VIS (in dichloromethane): 575 nm (ε 650 dm^3 mol^{-1} cm^{-1}). Positive-ion FAB mass spectrum: $m/z = 629$, M^+ [Found (Calc. for C$_{57}$H$_{57}$BClCoN$_3$O$_6$: C, 69.63 (69.48); H, 5.51 (5.83); N, 4.28 (4.26)%].

[CoL(H$_2$O)$_2$(NO$_3$)]BPh$_4$ 2. To a stirred solution of L (0.20 g, 0.4 mmol) and cobalt(II) nitrate hexahydrate (0.12 g, 0.4 mmol) in ethanol (50 cm^3) was added dropwise a solution of sodium tetraphenylborate (0.14 g, 0.4 mmol) in ethanol (10 cm^3). The salmon pink precipitate was filtered off under vacuum, washed with ethanol (50 cm^3) and desiccated until dry, darkening to purple (0.15 g, 0.14 mmol, 35%), m.p. 217.5–218 °C. IR (KBr pressed pellet): 3600–3400m (br), 3060w, 3000w, 2995w, 2900w, 1630s, 1590s, 1470w, 1455w, 1410w, 1255m, 1170m, 1155w, 980w, 945w, 750s, 745s, 680s, 675s, 605m, 550w and 505w cm^{-1}. UV/VIS (in dichloromethane): 546 nm (ε 440 dm^3 mol^{-1} cm^{-1}). Positive-ion FAB mass spectrum: $m/z = 592$, M^+ [Found (Calc. for C$_{57}$H$_{57}$BCoN$_4$O$_5$: C, 72.66 (72.23); H, 5.65 (6.06); N, 6.01 (5.91)%].

[CoL(Cl)]BPh₄ 3. To a stirred solution of L (0.20 g, 0.4 mmol) and cobalt(II) chloride hexahydrate (0.10 g, 0.4 mmol) in methanol (50 cm³) was added dropwise a solution of sodium tetraphenylborate (0.14 g, 0.4 mmol) in methanol (10 cm³). The blue precipitate was filtered off under vacuum, washed with methanol (50 cm³) and desiccated until dry (0.30 g, 0.3 mmol, 85%), m.p. 226–228 °C. IR (KBr pressed pellet): 3050w, 3025w, 3000w, 2950w, 1635s, 1600m, 1595s, 1460w, 1440w, 1420w, 1400w, 1250w, 1185s, 1130m, 1000w, 950w, 750s, 745s, 680s, 675s, 605s, 550w and 505m cm⁻¹. UV/VIS (in dichloromethane): 591 nm (ε 910 dm³ mol⁻¹ cm⁻¹). Positive-ion FAB mass spectrum: m/z = 565, M^+ [Found (Calc. for $C_{57}H_{53}BClCoN_3$: C, 77.21 (77.34); H, 5.86 (6.03); N, 5.13 (4.75)%].

[CoL(Br)]BPh₄ 4. To a stirred solution of L (0.20 g, 0.4 mmol) and cobalt(II) bromide hydrate (0.09 g, 0.4 mmol) in methanol (50 cm³) was added dropwise a solution of sodium tetraphenylborate (0.14 g, 0.4 mmol) in methanol (10 cm³). The blue precipitate was filtered off under vacuum, washed with methanol (50 cm³) and desiccated until dry (0.32 g, 0.3 mmol, 85%), m.p. 238–239 °C. IR (KBr pressed pellet): 3050w, 3025w, 3000w, 2950w, 1635s, 1600m, 1595s, 1460w, 1440w, 1420w, 1400w, 1250w, 1185s, 1130m, 1000w, 950w, 750s, 745s, 680s, 675s, 605s, 550w and 505m cm⁻¹. UV/VIS (in dichloromethane): 606 nm (ε 860 dm³ mol⁻¹ cm⁻¹). Positive-ion FAB mass spectrum: m/z = 610, M^+ [Found (Calc. for $C_{57}H_{53}BBrCoN_3$: C, 73.98 (73.64); H, 5.75 (5.75); N, 4.97 (4.52)%].

[CoL(I)]BPh₄ 5. To a stirred solution of L (0.20 g, 0.4 mmol) and cobalt(II) iodide (0.13 g, 0.4 mmol) in methanol (50 cm³) was added dropwise a solution of sodium tetraphenylborate (0.14 g, 0.4 mmol) in methanol (10 cm³). The green precipitate was filtered off under vacuum, washed with methanol (50 cm³) and desiccated until dry (0.31 g, 0.3 mmol, 80%), m.p. 239.5–240 °C. IR (KBr pressed pellet): 3050w, 3025w, 3000w, 2950w, 1635s, 1600m, 1595s, 1460w, 1440w, 1420w, 1400w, 1250w, 1185s, 1130m, 1000w, 950w, 750s, 745s, 680s, 675s, 605s, 550w and 505m cm⁻¹. UV/VIS (in dichloromethane): 604 nm (ε 910 dm³ mol⁻¹ cm⁻¹). Positive-ion FAB mass spectrum: m/z = 657, M^+ [Found (Calc. for $C_{57}H_{53}BCoIN_3$: C, 71.33 (70.09); H, 5.47 (5.47); N, 4.60 (4.30)%]. High-resolution positive-ion FAB mass spectrum: m/z = 657.1043 {Calc. for [CoL(I)]⁺ 657.1051}.

[(CoL)₂(µ-CO₃)][BPh₄]₂ 9. A solution of complex **1** or **2** (0.02 mmol) in dichloromethane (25 cm³) was shaken with sodium hydroxide pellets (1.85 g, 46.2 mmol) until the change in electronic spectrum shown in Fig. 3 was achieved. We propose this species (λ_{max} = 551 nm, ε = 428 dm³ mol⁻¹ cm⁻¹) to be [CoL-(OH)]⁺ **8**. Following filtration, carbon dioxide was bubbled through this solution for 5 min and it was then sealed and allowed to precipitate **9**, a purple solid, which was filtered off under vacuum and desiccated until dry (0.015 g, 0.01 mmol, 85%), m.p. 258–258.5 °C. IR (KBr pressed pellet): 2295m, 1610s, 1590s, 1540w, 1460w, 1440w, 1420w, 1400w, 1350w, 1250w, 1185s, 1105s, 1000m, 750s, 745s, 680s, 675s, 605s, 550w and 505m cm⁻¹ [Found (Calc. for $C_{115}H_{106}B_2Co_2N_6O_3$: C, 78.36 (78.50); H, 6.06 (6.07); N, 4.91 (4.78)%].

[CoL(OR)]⁺ (R = Me 6 or Et 7). Combination of complex **8** with an excess of the appropriate dapc in dichloromethane resulted in the production of **6** and **7**. The compounds were characterized in solution by positive-ion FAB mass spectrometry, UV/VIS and resonance-Raman spectroscopy. The mass spectra were taken in the presence of an equimolar quantity of an authentic sample of **3**, the molecular ions which resulted being of approximately equal intensity, m/z = 561 (**6**) and 575 (**7**) compared to m/z = 565 from **3**. UV/VIS (in dichloromethane): 549 (**6**), 548 nm (**7**), ε = 360 dm³ mol⁻¹ cm⁻¹. Resonance-Raman: 1634s, 1597m, 1269m, 1176s, 1000m with ν(C–O) 918s, ν(Co–O) 521w for **6**; ν(C–O) 900s, ν(Co–O) 520w for **7**.

Kinetics

Single-substrate reactions were monitored by a gas-evolution method,[26] mixed-substrate reactions by ¹H NMR spectroscopy and GC-EIMS. Gas-evolution measurements were performed in a stirred, jacketed water-bath. The reaction vessel, a 25 cm³ round-bottomed flask, was stirred at 700 revolutions min⁻¹ (above *ca.* 500 the rate was independent of stirrer speed) by a magnetic flea. The rate of reaction was followed by monitoring the gas evolution over 10–30 min (<10% reaction) with two gas syringes (100 cm³) attached to the reaction vessel *via* a two-way tap.

Catalytic rate constants, k_{obs} were obtained at 293.0(5) K with an approximately 1000-fold excess of dapc over complex: [dmpc] = 3.0, [depc] = 2.9 mol dm⁻³. Complex concentrations were in the range $(3–8) \times 10^{-4}$ mol dm⁻³ for dmpc and $(5–11) \times 10^{-4}$ mol dm⁻³ for depc. A combined plot for both substrates is shown in Fig. 7. Arrhenius parameters were obtained with a 1000-fold excess of dapc over complex, with a complex concentration of 1.0×10^{-5} mol dm⁻³. Temperatures were in the range 288–301 K: at lower temperatures gas evolution became impractically slow to be monitored by this method and at higher temperatures interference from solvent evaporation made this method unreliable. A combined plot for both substrates is shown in Fig. 10.

Uncatalysed reactions were conducted in CD_2Cl_2, scaled down to 5 cm³, and followed by ¹H NMR spectroscopy over several weeks. The conversions of dmpc [δ 3.80 (s, 6 H, CH₃)] into (MeO)₂CO [δ 3.66 (s, 6 H, CH₃)] and depc [δ 4.23 (q, 4 H, J = 7.0, CH₂) and 1.25 (t, 6 H, J = 7.0 Hz, CH₃)] into (EtO)₂CO [δ 4.07 (q, 4 H, J = 7.3, CH₂) and 1.18 (t, 6 H, J = 7.3 Hz, CH₃)] were extremely slow and less than 5% of the dapc was converted into dialkyl carbonate in this period of time. From this we can estimate a second-order rate constant for the decomposition of $\approx 10^{-10}$ dm³ mol⁻¹ s⁻¹ for dmpc and $\approx 10^{-8}$ dm³ mol⁻¹ s⁻¹ for depc.

Mixed-substrate reactions were conducted in CD_2Cl_2 and followed by ¹H NMR spectroscopy. The conversions of dmpc and depc into (MeO)₂CO and (EtO)₂CO respectively were monitored as above and the conversion into (MeO)(EtO)CO [δ 4.06 (q, 2 H, J = 7.3, CH₂), 3.64 (s, 3 H, CH₃) and 1.18 (t, 3 H, J = 7.3 Hz, CH₃)] was also observed. Final product distributions were confirmed by GC-EIMS: (MeO)₂CO, m/z 90 (M^+), 59, 45, 31 and 15; (MeO)(EtO)CO, 104 (M^+), 89, 77, 59, 45, 29 and 15; (EtO)₂CO, 118 (M^+), 91, 63, 45, 29 and 15.

Crystallography

Crystal data for complex 3. $C_{57}H_{53}BClCoN_3$, M = 885.21, monoclinic, space group $P2_1/c$, a = 15.593(1), b = 16.550(4), c = 19.947(6) Å, β = 109.495(14)°, U = 4852(2) Å³, Z = 4, D_c = 1.21 g cm⁻³, $F(000)$ = 1860. Blue blocks. Crystal dimensions: $0.70 \times 0.25 \times 0.25$ mm.

Crystals were mounted on a glass filament and sealed in epoxy adhesive. Rigaku AFC6S diffractometer, 293(2) K, ω–2θ scan mode, ω-scan speed 4.0° min⁻¹, graphite-monochromated Mo-Kα radiation, 7251 reflections measured (2.69 ⩽ θ ⩽ 25.00°, −23 < h < 22, 0 < k < 19, 0 < l < 16), 6628 unique, absorption correction applied (maximum, minimum transmission factors = 1.000, 0.954). Solution by Patterson methods with SAPI 91.[27] Full-matrix least-squares refinement on F^2 with SHELXL 93 [28] with all non-hydrogen atoms anisotropic and hydrogens refined using a riding model. Final R_F, wR_I values on all data were 0.146 and 0.134, and R_F, wR_I values on [$I_o > 2\sigma(I_o)$] data were 0.052 and 0.103; goodness of fit on F^2 = 1.006. Other programs used are given in ref. 29.

CCDC reference number 186/698.

References

1 D. C. Bradley, R. C. Mehrota and D. P. Gaur, *Metal Alkoxides*, Academic Press, New York, 1978.

2 R. A. Bartlett, J. J. Ellison, P. P. Power and S. C. Shoner, *Inorg. Chem.*, 1991, **30**, 2888 and refs. therein.

3 E. Kimura, Y. Kodama, T. Koike and M. Shiro, *J. Am. Chem. Soc.*, 1995, **117**, 8304.

4 M. J. Young, D. Wahnon, R. C. Hynes and J. Chin, *J. Am. Chem. Soc.*, 1995, **117**, 9441.

5 R. W. Adams, E. Bishop, R. L. Martin and G. Winter, *Aust. J. Chem.*, 1996, **19**, 207.

6 R. K. Dubey, A. Singh and R. C. Mehrotra, *Inorg. Chim. Acta*, 1988, **143**, 169.

7 F. A. Cotton and G. Wilkinson, *Advanced Inorganic Chemistry*, Wiley-Interscience, New York, 5th edn., 1988.

8 S. Ašperger and B. Cetina-Čižmek, *Inorg. Chem.*, 1996, **35**, 5232 and refs. therein.

9 P. Sobota, P. Utko, Z. Janas and S. Szafert, *Chem. Commun.*, 1996, 1923.

10 M. H. Chisholm and N. W. Eilerts, *Chem. Commun.*, 1996, 853.

11 L. Matilainen, M. Klinga and M. Leskelä, *J. Chem. Soc., Dalton Trans.*, 1996, 219.

12 B. Greener, M. H. Moore and P. H. Walton, *Chem. Commun.*, 1996, 27.

13 J. W. Egan, jun., B. S. Haggerty, A. L. Rheingold, S. C. Sendlinger and K. H. Theopold, *J. Am. Chem. Soc.*, 1990, **112**, 2445.

14 C. W. Li and R. C. Rosenberg, *J. Inorg. Biochem.*, 1993, **51**, 727.

15 H. Genth, *Gordian*, 1971, **71**, 255.

16 N. Sugeno (Sony Corp.), *Eur. Pat. Appl.*, EP 627 780 (*Chem. Abstr.*, 1995, **122**, 270 041n).

17 M. Ruf, F. A. Shell, R. Walz and H. Vahrenkamp, *Chem. Ber.*, 1997, **130**, 101.

18 R. Alsfasser, S. Trofimenko, H. Vahrenkamp and M. Ruf, *Chem. Ber.*, 1993, **126**, 703.

19 Kh. Sh. Khariton, M. E. Sohkevich, L. V. Kurtev and A. A. Shamshurin, *Zh. Prikl. Khim.*, 1969, **42**, 236.

20 A. S. Kovacs and H. O. Wolf, *Ind. Obst.-Gemueseverwert.*, 1963, **48**, 229.

21 C. K. Johnson, ORTEP, Report ORNL-5138, Oak Ridge National Laboratory, Oak Ridge, TN, 1976.

22 L. Cronin, B. Greener, M. H. Moore and P. H. Walton, *J. Chem. Soc., Dalton Trans.*, 1996, 3337.

23 H. Stetter and J. Bremen, *Chem. Ber.*, 1973, **106**, 2523.

24 N. Kitajima, S. Hikichi, M. Tanaka and Y. Moro-Oka, *J. Am. Chem. Soc.*, 1993, **115**, 5496; M. Ruf and H. Vahrenkamp, *Inorg. Chem.*, 1996, **35**, 6571.

25 F. Lions and K. V. Martin, *J. Am. Chem. Soc.*, 1957, **79**, 1572.

26 V. I. Kovalenko, *Zh. Obschei. Khim.*, 1952, **22**, 1546.

27 F. Hai-Fu, SAPI 91, structure analysis programs with intelligent control, Rigaku Corporation, Tokyo, 1993.

28 G. M. Sheldrick, SHELXL 93, program for crystal structure refinement, University of Göttingen, 1993.

29 P. T. Beurskens, G. Admiraal, G. Beurskens, W. P. Bosman, S. Garcia-Granda, R. O. Gould, J. M. M. Smits and C. Smykalla, The DIRDIF program system, Technical report of the crystallography laboratory, University of Nijmegen, 1992.